AIMS Mathematics, 11(3): 6269–6296.
DOI: 10.3934/math.2026259
Received: 27 November 2025
Revised: 25 February 2026
Accepted: 03 March 2026
Published: 12 March 2026

https://www.aimspress.com/journal/Math

Research article

The modified Muth distribution: Statistical properties, entropy measures, and parameter estimation

H. M. Barakat[1], H. S. Bakouch[2], Mohamed A. Abd Elgawad[3,*], Hatem Semary[3], M. A. Alawady[1,4], I. A. Husseiny[1], M. G. Enany[5] and T. S. Taher[1]

[1] Department of Mathematics, Faculty of Science, Zagazig University, Zagazig 44519, Egypt

[2] Department of Mathematics, Faculty of Science, Tanta University, Tanta, Egypt

[3] Department of Mathematics and Statistics, Faculty of Science, Imam Mohammad Ibn Saud Islamic University (IMSIU), Riyadh 11432, Saudi Arabia

[4] Department of Statistics and Operations Research, College of Science, Qassim University, Buraydah 51482, Saudi Arabia

[5] Faculty of Computers and Information Systems, Egyptian Chinese University, Cairo 11528, Egypt

* **Correspondence:** Email: moaasalem@imamu.edu.sa.

Abstract: In this study, the modified Muth distribution was introduced as a parsimonious lifetime model obtained by structurally modifying the Muth survival function. The proposed construction preserves the scale-family property while altering tail behavior and cumulative hazard growth. A statistical analysis was presented, including derivations of moments, the moment-generating function, and several entropy measures. Parameter estimation was carried out using maximum likelihood, and interval estimation was performed via the Fisher information matrix. The performance of the model was examined through extensive simulation studies and a real-world data application involving strength measurements of carbon fibers. In this application, the modified Muth distribution provides a competitive and, in several cases, improved fit compared with commonly used lifetime models.

Keywords: Muth distribution; exponential-type models; information measures; maximum likelihood estimation; reliability data
Mathematics Subject Classification: 60B12, 62G30

1. Introduction and preliminary results

Parsimonious probability distributions strike a good balance between model flexibility and simplicity in parameters. Parsimonious probability distributions with fewer parameters reduce the risk

of overfitting and often provide more stable inference, see ([1], Chapter 2). This focus on simplicity not only makes interpretation clearer but also enhances generalization to diverse data, providing robust tools for analysis.

Among the distributions that exemplify this principle, the Muth distribution is a key example of a one-parameter lifetime distribution introduced by Muth [2]. It has garnered attention for modeling reliability phenomena. Its cumulative distribution function (CDF) is defined as follows:

$$F_Y(y;\alpha) = 1 - \exp[\alpha y - \frac{1}{\alpha}(e^{\alpha y} - 1)], \quad y > 0, \tag{1.1}$$

where $\alpha \in (0, 1]$ is a shape parameter. By setting $\alpha = 1$ in (1.1) and incorporating a scale parameter $\beta > 0$, we obtain the scaled Muth distribution (also called the baseline Muth distribution), denoted by $F_0(x;\beta)$, with the CDF:

$$F_0(x;\beta) = 1 - \exp\left[\frac{x}{\beta} - \left(e^{x/\beta} - 1\right)\right], \quad x > 0,\ \beta > 0. \tag{1.2}$$

When $\beta = 1$, this reduces to the canonical baseline Muth distribution with the CDF: $F_0(x) := F_0(x; 1)$.

The Muth distribution is noted for several properties: (i) its probability density function (PDF) exhibits a lighter right tail compared to standard gamma, log-normal, and Weibull distributions; and (ii) it has sufficient flexibility to fit certain lifetime datasets well, especially those from reliability experiments [2–4]. Note that some other features of the Muth distribution (such as limiting exponential behavior and specific generation properties) do not carry over to the modified version introduced below.

Recent advances in reliability engineering and survival analysis have yielded the development of sophisticated modeling techniques that capture complex degradation processes and distributional uncertainty. For instance, He et al. [5] proposed a physics-informed neural network-supported Wiener process for degradation modeling and reliability prediction, demonstrating the value of integrating machine learning with traditional stochastic processes. In a related direction, He et al. [6] developed an artificial neural network-supported Tweedie exponential dispersion process, while He et al. [7] introduced a nonparametric degradation modeling approach that explicitly accounts for distribution uncertainty through B-spline functions. These developments highlight the growing need for flexible yet interpretable models that can accommodate diverse data characteristics. Within this context, the proposed modified Muth (MMuth) distribution offers a parsimonious parametric alternative that preserves analytical tractability while providing enhanced tail flexibility and monotone aging behavior, making it particularly suitable for reliability applications where model simplicity and interpretability are paramount.

To improve modeling options for this family of distributions, this paper introduces the modified Muth (MMuth) distribution. Its CDF is defined as:

$$F(x;\theta) = 1 - \frac{1 + \exp[\frac{2x}{\theta}]}{2} \exp[-(e^{\frac{x}{\theta}} - 1)], \quad x > 0,\ \theta > 0.$$

From this point onward, we note that the MMuth distribution forms a scale family. Accordingly, all distributional and shape-related properties can be developed without loss of generality in the canonical case $\theta = 1$. Results for a general scale parameter $\theta > 0$ follow immediately by standard scaling arguments.

The CDF of the canonical MMuth distribution is defined as

$$F(x) = 1 - \frac{1 + \exp(2x)}{2} \exp[-(e^x - 1)], \quad x > 0. \tag{1.3}$$

Differentiating (1.3), the corresponding probability density function (PDF) is obtained as

$$f(x) = \frac{1}{2}(e^x - 1)^2 \exp(x - (e^x - 1)), \quad x > 0. \tag{1.4}$$

Proposition 1.1. *The function (1.4) is a valid PDF. As $x \to \infty$,*

$$f(x) \sim \frac{e}{2} \exp(3x - e^x),$$

which shows that $f(x)$ decreases faster than any exponential function e^{-cx} and is therefore integrable.

Proof. First, note that $f(x) > 0$ for all $x > 0$. Using the substitution $y = e^x - 1$ (so that $dy = e^x\,dx = (y + 1)\,dx$), we obtain

$$\int_0^\infty f(x)\,dx = \frac{1}{2}\int_0^\infty y^2 e^{-y}\,dy = \frac{1}{2}\,\Gamma(3) = 1.$$

Hence $f(x)$ integrates to one and is therefore a valid PDF.

To study the tail behavior, we rewrite the density as

$$f(x) = \frac{e}{2}(e^x - 1)^2 e^x e^{-e^x}.$$

As $x \to \infty$, $(e^x - 1)^2 \sim e^{2x}$, yielding

$$f(x) \sim \frac{e}{2} \exp(3x - e^x),$$

which completes the proof. □

The survival function (SRF) of the canonical MMuth distribution is

$$S(x) = \frac{1 + \exp(2x)}{2} \exp[-(e^x - 1)], \quad x > 0. \tag{1.5}$$

The hazard rate function (HRF) of the canonical MMuth distribution is

$$H(x) = \frac{(e^x - 1)^2 \exp(x)}{1 + \exp(2x)} = \frac{1}{2}\frac{(e^x - 1)^2}{\cosh(x)}, \quad x > 0. \tag{1.6}$$

Proposition 1.2. *The HRF (1.6) is increasing in x.*

Proof. Differentiating $H(x)$ with respect to x and simplifying shows that the derivative is positive for all $x > 0$, which establishes the increasing nature of the HRF. □

Figure 1 graphically illustrates the PDF, CDF, SRF, and HRF of the MMuth distribution at $\theta = 1$ in comparison with the Muth distribution for $\alpha = 0.5$ and $\alpha = 1$. The MMuth density is more sharply peaked, indicating greater concentration around the mode. The corresponding CDF increases more rapidly, implying larger cumulative probabilities for fixed x, while the SRF decays faster, reflecting

reduced survival probabilities and lighter tail behavior. Moreover, the HRF is monotonically increasing for all models, confirming the aging property proved analytically; however, the MMuth hazard rate increases more steeply, particularly for moderate to large values of x, indicating stronger wear-out behavior. Overall, these graphical patterns corroborate the theoretical results to follow and demonstrate that the MMuth distribution provides an effective alternative to the classical Muth model for modeling lifetime data with accelerated failure characteristics.

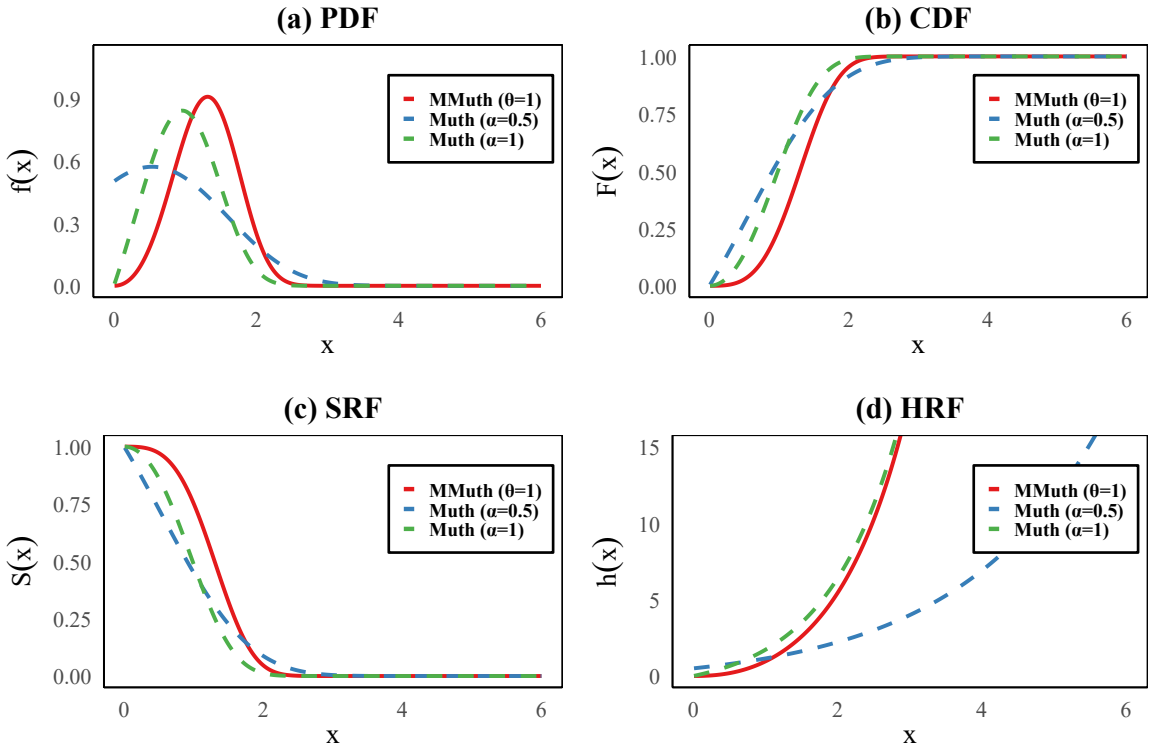

Figure 1. Plots of PDF, CDF, SRF, and HRF of the MMuth distribution ($\theta = 1$) and the Muth distribution ($\alpha = 0.5, 1$).

1.1. Structural motivation and relationship to existing Muth-type models

The MMuth distribution is a part of the scale families, which offers several statistical benefits despite having fixed shape characteristics. Scale families provide theoretical simplicity, better interpretability, and strong estimation procedures. The main benefits of the MMuth distribution include:

- Theoretical simplicity: All distribution properties come from the standard form ($\theta = 1$).
- Moment relationships: $\mu_r(\theta) = \theta^r \mu_r(1)$ for all moments.
- Quantile function: $Q(p;\theta) = \theta \cdot Q(p;1)$ for direct percentile calculations.
- CDF: $F(x;\theta) = F\left(\frac{x}{\theta};1\right)$ simplifies probability calculations.
- Scale-equivariant estimation: $\hat{\theta}(cX) = c\hat{\theta}(X)$ ensures consistent estimation.
- Hazard rate scaling: $H(x;\theta) = \frac{1}{\theta}H\left(\frac{x}{\theta};1\right)$ keeps the proportional hazard structure.
- Accelerated failure time: $S(x;\theta) = S\left(\frac{x}{\theta};1\right)$ naturally models the effect of covariates on lifetime.

These properties make the MMuth distribution very useful for reliability applications where the failure mechanism stays the same across various operating conditions, with only the time scale changing proportionally to θ.

Parsimonious lifetime distributions play a central role in reliability theory and survival analysis, where interpretability, analytical tractability, and numerical stability are often as important as goodness-of-fit [8]. The classical Muth distribution is a one-parameter model exhibiting monotone aging behavior. Still, its tail structure may be restrictive in applications involving heterogeneous environments or rare but severe failure events. Most existing extensions of the Muth distribution aim to increase flexibility through parameter augmentation, such as power transformations or additional shape parameters. While effective in certain contexts, these approaches increase model complexity and may obscure the physical interpretation of the parameters.

The MMuth distribution proposed in this paper adopts a fundamentally different construction strategy. Rather than enlarging the parameter space, the MMuth model is obtained through a structural modification of the SRF of a baseline Muth-type distribution. Since the MMuth distribution forms a scale family, the construction is presented without loss of generality in the canonical case $\theta = 1$.

Specifically, the MMuth SRF admits the multiplicative representation

$$S(x) = \omega(x)\, S_0(x), \qquad \omega(x) = \cosh(x), \tag{1.7}$$

where

$$S_0(x) = \exp[x - (e^x - 1)]$$

is the SRF of the corresponding baseline Muth distribution (1.2) in the canonical form. The representation in (1.7) places the MMuth model within the class of weighted or modified survival models [9, 10], with the distinctive feature that the weight function depends on the same argument as the baseline distribution.

Theoretical motivation for the weighting function. The weighting function $\omega(x) = \cosh x$ in representation (1.7) was selected for both mathematical and practical reasons. In the context of SRFs for positive random variables (RVs), a valid weighting function $\omega(x)$ must satisfy:

- $\omega(0) = 1$ to preserve the normalization $S(0) = S_0(0) = 1$;
- $\omega(x) \geq 0$ for all $x > 0$;
- $\omega(x)S_0(x)$ is decreasing in x and $\lim_{x\to\infty} \omega(x)S_0(x) = 0$.

The hyperbolic cosine function satisfies these conditions while offering several advantageous properties:

- It admits a simple closed form that facilitates the derivation of distributional properties.
- It yields an analytically tractable SRF (1.5) and HRF (1.6).
- The resulting distribution preserves the scale-family structure of the baseline Muth model.
- It produces a heavier-tailed distribution while maintaining monotone hazard rate behavior.

While alternative weighting functions (such as power or exponential forms) could be considered, the choice $\omega(x) = \cosh x$ leads to particularly elegant expressions for the MMuth distribution's key functions. Moreover, $\omega(x)$ is increasing, resulting in a different interpretation but one that nevertheless yields a valid lifetime distribution with useful properties for reliability modeling.

Proposition 1.3. *(Stochastic dominance) Let* $X \sim$ MMuth *and* $X_0 \sim$ Muth. *Then*

$$S(x) \geq S_0(x), \qquad x > 0,$$

or equivalently, $F(x) \leq F_0(x)$ *for all* $x > 0$. *Thus, the MMuth distribution dominates the Muth distribution in the usual stochastic order.*

Proof. For all $x > 0$, $\cosh(x) \geq 1$. Hence, $S(x) = \cosh(x)S_0(x) \geq S_0(x)$, which establishes the result. □

The above proposition shows that the MMuth model assigns uniformly larger survival probabilities than its baseline counterpart, providing a principled mechanism for modeling heavier-tailed lifetime behavior.

Proposition 1.4. *(Tail dominance) Let* $f(x)$ *and* $f_0(x)$ *denote the PDFs of the MMuth and Muth distributions, respectively. Then*

$$\lim_{x\to\infty} \frac{f(x)}{f_0(x)} = \infty,$$

and consequently the MMuth distribution has a heavier right tail than the Muth distribution.

Proof. From the explicit density expressions,

$$\frac{f(x)}{f_0(x)} = \frac{1}{2}(e^x - 1),$$

which diverges to infinity as $x \to \infty$. □

Aging property. Despite the increased tail weight, the MMuth distribution preserves monotone aging behavior.

Proposition 1.5. *(Increasing failure rate) The HRF of the MMuth distribution is strictly increasing; that is, the MMuth distribution belongs to the class of increasing-failure-rate (IFR) models. This implies that the failure intensity increases monotonically over time, reflecting a progressive aging or wear-out mechanism.*

Proof. Let $y = e^x > 1$. Then the HRF can be written as

$$H(x) = g(y), \text{ where } g(y) = \frac{(y-1)^2 y}{1+y^2}.$$

Since y is strictly increasing in x, it suffices to show that $g'(y) > 0$ for all $y > 1$. A straightforward calculation gives

$$g'(y) = \frac{y^4 + 2y^2 - 4y + 1}{(1+y^2)^2}.$$

For $y > 1$, the numerator is strictly positive and the denominator is positive for all $y > 0$. Hence $g'(y) > 0$ for all $y > 1$, which implies $H'(x) > 0$ for all $x > 0$. Therefore, the MMuth distribution belongs to the IFR class. □

Proposition 1.5 emphasizes that, due to this structural property, the MMuth distribution cannot exhibit non-monotone HRF shapes, such as bathtub or upside-down bathtub forms. Thus, the additional flexibility introduced by the SRF modification operates through tail behavior and stochastic dominance rather than through changes in hazard rate shape. This makes the MMuth model particularly suitable for reliability applications where monotone aging behavior is theoretically or empirically justified.

In addition, Propositions 1.3–1.5 collectively demonstrate that the MMuth distribution achieves controlled tail flexibility through a structurally motivated survival modification rather than parameter augmentation. The model preserves scale-family invariance and monotone aging behavior while allowing for heavier tails and delayed failures. These properties distinguish the MMuth distribution from multi-parameter Muth-type extensions and position it as a parsimonious and interpretable alternative for reliability and survival applications.

Scope and positioning. The objective of this work is to develop and study a parsimonious and analytically tractable lifetime distribution that competes with the classical Muth model while preserving its scale-family structure. The proposed MMuth distribution is intended as a flexible modeling tool for reliability and survival data, enabling improved representation of hazard-rate and tail behavior relative to the baseline model. While such modeling improvements may inform reliability assessment and risk interpretation, the present paper does not address decision-oriented optimization issues, such as maintenance scheduling or system-level resource allocation, which require additional modeling layers and data structures.

In this paper, the following contributions are presented: (i) the MMuth distribution is introduced and its main properties are derived, including the PDF, CDF, SRF, HRF, integral representations for moments, the moment-generating function (MGF), and tail and mode behavior; (ii) several information measures for the MMuth distribution are derived and analyzed, including Rényi, Tsallis, Havrda-Charvát, and Arimoto entropies, as well as extropy, which extend classical uncertainty summaries; (iii) a comprehensive estimation toolkit is examined, comprising maximum likelihood (ML), least squares (LS), weighted least squares (WLS), Cramér-von Mises (CvM), Anderson-Darling (AD), and maximum product spacing (MPS) methods, together with practical interval estimation procedures. For frequentist inference, estimator variability is quantified using the observed Fisher information (FI), leading to asymptotic confidence intervals (CIs); when closed-form expected information is unavailable, the observed information is computed numerically; (iv) an extensive Monte Carlo study is conducted to assess estimator stability across varying sample sizes and parameter configurations; and (v) the MMuth model is applied to a real-world dataset (glass-fiber strengths), where it achieves competitive and, in several cases, improved fits relative to several two- and three-parameter alternatives based on multiple information criteria and goodness-of-fit measures. Overall, these results demonstrate that the MMuth distribution preserves parsimony while accommodating a broad range of lifetime and reliability behaviors.

The rest of the paper is organized as follows. Section 2 examines properties of the MMuth distribution, including moments, the MGF, reliability functions, and information measures. Section 3 outlines estimation procedures and interval estimation (ML, MPS, LS, WLS, CvM, and AD methods). Section 4 presents the Monte Carlo study and summarizes estimator performance. Section 5 applies the MMuth distribution to a real-world dataset and compares results with various competitors. Section 6 wraps up the paper and suggests ideas for future work.

2. Properties of the model

2.1. Moments and the moment generating function

The following proposition gives the rth moment of the MMuth distribution.

Proposition 2.1. *For real $r > -3$, the rth moment of the MMuth distribution with $\theta = 1$ is*

$$\mu_r = \frac{1}{2}\int_0^\infty [\log(1+y)]^r y^2 e^{-y}\,\mathrm{d}y.$$

Proof. Using the change of variable $y = e^x - 1$, i.e., $x = \log(1+y)$, the rth moment is obtained as

$$\begin{aligned}\mu_r &= \int_0^\infty x^r f(x)\,\mathrm{d}x = \int_0^\infty x^r \frac{1}{2}(e^x-1)^2 \exp[x-(e^x-1)]\,\mathrm{d}x \\ &= \int_0^\infty [\log(1+y)]^r \frac{1}{2} y^2 \exp[\log(1+y)-y]\frac{1}{1+y}\,\mathrm{d}y \\ &= \frac{1}{2}\int_0^\infty [\log(1+y)]^r y^2 e^{-y}\,\mathrm{d}y.\end{aligned}$$

It remains to prove that the integral $\int_0^\infty [\log(1+y)]^r y^2 e^{-y}\,\mathrm{d}y$ is absolutely convergent. We split the integral at $y = 1$:

$$\int_0^\infty [\log(1+y)]^r y^2 e^{-y}\,\mathrm{d}y = \int_0^1 [\log(1+y)]^r y^2 e^{-y}\,\mathrm{d}y + \int_1^\infty [\log(1+y)]^r y^2 e^{-y}\,\mathrm{d}y.$$

For $y \to 0$, we use $\log(1+y) = y - y^2/2 + O(y^3)$. Hence there exist $c \in (0,1)$ and $C_1 > 0$ such that for all $0 \le y \le c$, $\frac{y}{2} \le \log(1+y) \le 2y$. Consequently, for $0 \le y \le c$, $[\log(1+y)]^r y^2 e^{-y} \le C_1 y^{r+2}$. Since $r+2 > -1$ (i.e., $r > -3$), the function $y \mapsto y^{r+2}$ is integrable on $[0, c]$. Thus $\int_0^c [\log(1+y)]^r y^2 e^{-y}\,\mathrm{d}y < \infty$. For large y, $\log(1+y) \sim \log y$. Fix $0 < \varepsilon < 1$. For every real r,

$$\lim_{y\to\infty} \frac{(\log y)^{|r|}}{e^{\varepsilon y}} = 0,$$

so there exist $Y \ge 1$ and $C_2 > 0$ such that for all $y \ge Y$, $[\log(1+y)]^r \le C_2 e^{\varepsilon y}$. Hence for $y \ge Y$, $[\log(1+y)]^r y^2 e^{-y} \le C_2\, y^2 e^{-(1-\varepsilon)y}$, which is integrable on $[Y, \infty)$ because of the exponential decay. Adding the finite piece $\int_c^Y$ (a continuous integrand on a compact interval) gives $\int_0^\infty [\log(1+y)]^r y^2 e^{-y}\,\mathrm{d}y < \infty$ for all $r > -3$. □

Applying the substitution $t = \log[1+y]$, yields

$$\mu_r = \frac{e}{2}\int_0^\infty t^r \left[e^{3t-e^t} - 2e^{-e^t+2t} + e^{-e^t+t}\right]\mathrm{d}t, \qquad r > -3.$$

In particular, the first four moments for $\theta = 1$ are

$$\mu_1 = 1.298174, \quad \mu_2 = 1.862313, \quad \mu_3 = 2.877279, \text{ and } \mu_4 = 4.714074.$$

The variance is

$$\sigma^2 = \mu_2 - \mu_1^2 = 1.862313 - (1.298174)^2 \approx 0.17706.$$

The skewness τ_1, kurtosis τ_2, and coefficient of variation τ_3 for the MMuth distribution are

$$\tau_1 = \frac{\mu_3 - 3\mu_1\mu_2 + 2\mu_1^3}{\sigma^3} = -0.0003972 \text{ (almost, the CDF is symmetric)},$$

$$\tau_2 = \frac{\mu_4 - 4\mu_1\mu_3 + 6\mu_2\mu_1^2 - 3\mu_1^4}{\sigma^4} = 2.67375,$$

$$\tau_3 = \frac{\sigma}{\mu_1} = 0.324134.$$

The MGF is

$$\begin{aligned} M(t) &= \int_0^\infty e^{xt} f(x)\,\mathrm{d}x = \int_0^\infty e^{xt}\,\frac{1}{2}\,(e^x-1)^2 \exp[x-(e^x-1)]\,\mathrm{d}x \\ &= \int_0^\infty (1+y)^t\,\frac{1}{2}\,y^2\,\exp[\log(1+y)-y]\,\frac{1}{1+y}\,\mathrm{d}y = \frac{1}{2}\int_0^\infty (1+y)^t\,y^2 e^{-y}\,\mathrm{d}y. \end{aligned}$$

Let $1 + y = x$. Then

$$M(t) = \frac{e}{2}\int_1^\infty x^t\,(x-1)^2\,e^{-x}\,\mathrm{d}x = \frac{e}{2}\int_1^\infty [x^{t+2} - 2x^{t+1} + x^t]e^{-x}\,\mathrm{d}x.$$

Using the upper incomplete gamma function $\Gamma(a,1) = \displaystyle\int_1^\infty x^{a-1}e^{-x}\,\mathrm{d}x$, we obtain

$$M(t) = \frac{e}{2}\,[\Gamma(t+3,1) - 2\Gamma(t+2,1) + \Gamma(t+1,1)].$$

Let $m = t+1$. Employing the recurrence $\Gamma(a+1,1) = a\Gamma(a,1) + e^{-1}$, we get $\Gamma(m+1,1) = m\Gamma(m,1) + e^{-1}$ and

$$\Gamma(m+2,1) = (m+1)\Gamma(m+1,1) + e^{-1} = m(m+1)\Gamma(m,1) + (m+2)e^{-1}.$$

Hence, $\Gamma(m+2,1) - 2\Gamma(m+1,1) + \Gamma(m,1) = (m^2 - m + 1)\Gamma(m,1) + me^{-1}$. Substituting back $m = t+1$ yields

$$\Gamma(t+3,1) - 2\Gamma(t+2,1) + \Gamma(t+1,1) = (t^2+t+1)\Gamma(t+1,1) + (t+1)e^{-1}.$$

Therefore, the MGF simplifies to

$$M(t) = \frac{1}{2}\,[e\,(t^2+t+1)\,\Gamma(t+1,1) + t + 1].$$

From the CDF of the MMuth distribution with $\theta = 1$, the median m_1 satisfies $F(m_1) = 0.5$, i.e.,

$$(1 + e^{2m_1})e^{-(e^{m_1}-1)} = 1.$$

Setting $u = e^{m_1}$ gives $e^{u-1} = 1 + u^2$. The numerical solution yields $u \approx 3.6736$, hence $m_1 = \log u \approx 1.301$. We observe that the mean-to-median ratio is $1.298/1.301 \approx 0.998$, which is very close to one.

2.2. Mean residual life, cumulative hazard, and reversed hazard

For the MMuth distribution, the SRF (with $y = e^x$) is

$$S(x) = \frac{1+y^2}{2}\, e^{-(y-1)}.$$

The mean residual life (MRL) at time x is

$$m(x) = \mathbb{E}[X - x \mid X > x] = \frac{1}{S(x)} \int_x^\infty S(t)\, \mathrm{d}t.$$

Using the change of variable $y = e^t$,

$$\int_x^\infty S(t)\, \mathrm{d}t = \frac{1}{2}\Big[e\, E_1(y) + (y+1)e^{\,1-y}\Big], \qquad y = e^x.$$

Hence the MRL simplifies to

$$m(x) = \frac{e^y E_1(y) + (y+1)}{1+y^2}, \qquad y = e^x. \tag{2.1}$$

Here $E_1(z) = \int_z^\infty t^{-1} e^{-t}\, \mathrm{d}t$ is the exponential integral.

The cumulative hazard (integrated hazard) is

$$\Lambda(x) = \int_0^x H(u)\, \mathrm{d}u = y - 1 - \log\Big(\frac{1+y^2}{2}\Big), \qquad y = e^x.$$

The reversed hazard (backward hazard) is

$$\bar{r}(x) = \frac{f(x)}{F(x)} = \frac{1}{2}\, \frac{y\,(y-1)^2}{2e^{y-1} - (1+y^2)}, \qquad y = e^x.$$

The reversed hazard is algebraic in y and straightforward to evaluate numerically; it is useful for backward-time analyses or left-tail risk measures.

Consistency with the mean. Setting $x = 0$ (so that $y = e^0 = 1$) in (2.1) gives

$$m(0) = \frac{eE_1(1) + 2}{2}.$$

For the canonical MMuth distribution ($\theta = 1$), the unconditional mean μ_1 was obtained in Proposition 7 as $\mu_1 \approx 1.298174$. Using the value $E_1(1) \approx 0.2193839$, we compute

$$\frac{e \times 0.2193839 + 2}{2} \approx 1.298174,$$

which confirms that $m(0) = \mu_1$. For a general scale parameter $\theta > 0$, the MRL at zero scales accordingly:

$$m(0;\theta) = \theta\, m(0;1) = \theta\, \mu_1 = \mu_1(\theta).$$

Thus, the MRL at zero indeed equals the unconditional mean.

Figure 2 displays the MRL function $m(x)$, the cumulative hazard function $\Lambda(x)$, and the reversed hazard rate $\bar{r}(x)$ of the MMuth distribution in the canonical case $\theta = 1$. The strictly decreasing behavior of $m(x)$ indicates a monotone aging mechanism. The cumulative hazard function is increasing and convex, which is consistent with the IFR property established analytically. Moreover, the reversed hazard rate exhibits a rapid decrease, highlighting the relatively heavier right-tail behavior of the MMuth distribution.

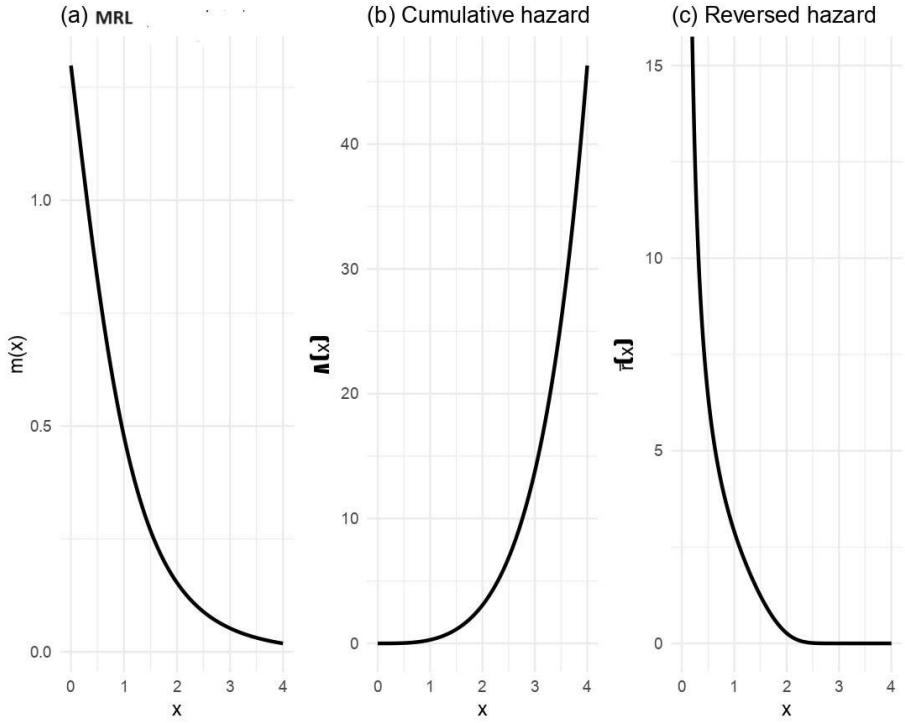

Figure 2. Plots of (a) MRL $m(x)$, (b) cumulative hazard $\Lambda(x)$, and (c) reversed hazard $\bar{r}(x)$ for the MMuth distribution.

2.3. Some entropy measures

Entropy measures the uncertainty or randomness in an RV. It is a key idea in information theory and has many applications in physics, engineering, and applied sciences. For a thorough overview of generalized entropy measures, see [11, 12]. For an RV $X \sim$ MMuth(1), the Rényi entropy of order $1 \neq \delta > 0$ is defined as:

$$\varphi(X) = \frac{1}{1-\delta} \log \left\{ \int_0^\infty f^\delta(x) dx \right\}. \tag{2.2}$$

Proposition 2.2. *Let $X \sim$* MMuth(1)*. For any $\delta > 0$ with $\delta \neq 1$, the Rényi entropy of X is given by*

$$\varphi(X) = \frac{1}{1-\delta} \left[\delta(1 - \log 2) + \log \left(\sum_{m=0}^{\infty} \frac{(-1)^m \binom{2\delta}{m}}{\delta^{3\delta - m}} \Gamma(3\delta - m, \delta) \right) \right], \tag{2.3}$$

where the generalized binomial coefficient is defined by

$$\binom{2\delta}{m} = \frac{\Gamma(2\delta+1)}{m!\,\Gamma(2\delta-m+1)}.$$

If 2δ is a positive integer, the summation terminates at $m = 2\delta$.

Proof. From the definition of the Rényi entropy,

$$\varphi(X) = \frac{1}{1-\delta}\log R_\delta \text{ and } R_\delta = \int_0^\infty f^\delta(x)\,dx.$$

Using the PDF of the MMuth(1) distribution, we have

$$\begin{aligned} R_\delta &= \int_0^\infty \left[\frac{1}{2}(e^x-1)^2\exp(x-e^x+1)\right]^\delta dx \\ &= \frac{1}{2^\delta}\int_0^\infty (e^x-1)^{2\delta}\exp\Big(\delta\Big(x-e^x+1\Big)\Big)\,dx. \end{aligned}$$

Applying the generalized binomial expansion,

$$(e^x-1)^{2\delta} = \sum_{m=0}^{\infty}(-1)^m\binom{2\delta}{m}e^{(2\delta-m)x},$$

and performing the change of variable $y = e^x$, $dx = dy/y$, we obtain

$$R_\delta = \frac{e^\delta}{2^\delta}\sum_{m=0}^{\infty}(-1)^m\binom{2\delta}{m}\int_1^\infty y^{3\delta-m-1}e^{-\delta y}\,dy.$$

The integral evaluates to

$$\int_1^\infty y^{3\delta-m-1}e^{-\delta y}\,dy = \delta^{-(3\delta-m)}\Gamma(3\delta-m,\delta),$$

and therefore

$$R_\delta = e^\delta 2^{-\delta}\sum_{m=0}^{\infty}\frac{(-1)^m\binom{2\delta}{m}}{\delta^{3\delta-m}}\Gamma(3\delta-m,\delta). \tag{2.4}$$

Substituting this expression into $\varphi(X) = \frac{1}{1-\delta}\log R_\delta$ yields (2.3). □

The parameter δ controls how sensitive the entropy measure is to various parts of the probability distribution. As δ approaches 1, Rényi entropy becomes equal to Shannon entropy, which is the standard way to measure information. When δ equals 2, it turns into collision entropy, focusing on the most likely events. As δ approaches infinity, the measure increasingly reflects only the highest-probability events, effectively overlooking rare outcomes. This feature makes Rényi entropy especially valuable in situations where low-probability events can be ignored.

Lad et al. [13] proposed a measure of randomness of an RV called extropy. It can be viewed as a complement dual of Shannon entropy. Extropy and related information measures have since been

studied in various contexts, including concomitants and record values in [14–17]. Here, for $X \sim$ MMuth(1), the extropy of X is defined as

$$J(X) = -\frac{1}{2}\int_0^\infty f^2(x)dx = -\frac{1}{2}R_2.$$

Hence, based on (2.4), when $\delta = 2$, we can express it as

$$J(X) \quad = \quad -\frac{e^2}{8}\sum_{m=0}^{4}\frac{(-1)^m\binom{4}{m}}{2^{6-m}}\Gamma(6-m,2).$$

For the canonical case $\theta = 1$, the numerical value is $J(X) = -0.328125$. For general θ, $J(X;\theta) = -0.328125/\theta$.

Tsallis [18] proposed a generalized measure of randomness, known as the Tsallis entropy, defined by

$$S_\delta(X) = \frac{1}{1-\delta}\left[R_\delta - 1\right], \quad \delta > 0,\ \delta \neq 1.$$

Havrda and Charvát [19] proposed an extension of Rényi entropy, known as the Havrda–Charvát entropy, defined as

$$\mathcal{HC}_\delta(X) = \frac{1}{2^{1-\delta}-1}\left[R_\delta - 1\right], \quad \delta > 0,\ \delta \neq 1.$$

Arimoto [20] introduced another generalization of Shannon entropy, called the Arimoto entropy, defined by

$$A_\delta(X) = \frac{\delta}{1-\delta}\left[R_\delta^{1/\delta} - 1\right], \quad \delta > 0,\ \delta \neq 1.$$

These entropy measures provide complementary information about the uncertainty structure of the MMuth distribution and can be evaluated using the expression for R_δ in (2.4).

2.3.1. Interpretation and practical relevance of entropy measures

Entropy-based measures provide complementary information to classical moment-based summaries and play an important role in reliability and survival analysis by quantifying uncertainty, dispersion, and tail sensitivity in lifetime distributions. Unlike variance or higher-order moments, entropy measures capture the overall concentration of probability mass and are particularly sensitive to tail behavior, which is often critical in modeling rare, but severe failure events.

Generalized entropy measures, such as Rényi and Tsallis entropies allow for flexible weighting of different regions of the distribution through their tuning parameters. In the context of lifetime modeling, these measures are useful for assessing how uncertainty is distributed between early-life and late-life failures. Higher sensitivity to the right tail makes these entropies especially relevant for reliability systems where extreme lifetimes, delayed failures, or stress-strength considerations are of practical interest.

Havrda-Charvát and Arimoto entropies further extend this framework by emphasizing deviations from uniform uncertainty and by providing alternative quantifications of distributional concentration. These measures can be employed in comparative studies to assess how competing lifetime models differ in their uncertainty profiles, even when classical goodness-of-fit statistics yield similar conclusions.

Extropy, is a dual measure of Shannon entropy, focuses on the concentration of probability mass away from regions of high likelihood. In reliability applications, extropy is particularly useful for distinguishing models with similar central behavior but different tail decay properties. This makes it a valuable tool for comparative uncertainty analysis and model selection in lifetime data analysis.

In summary, the entropy measures derived in this section are not introduced merely as mathematical extensions, but as interpretable tools that provide additional insight into the uncertainty structure and tail characteristics of the MMuth distribution. Their inclusion enhances the understanding of the proposed model from both theoretical and applied reliability perspectives, complementing classical moment-based analyses.

Figure 3 shows how different entropy measures change with the parameter δ.

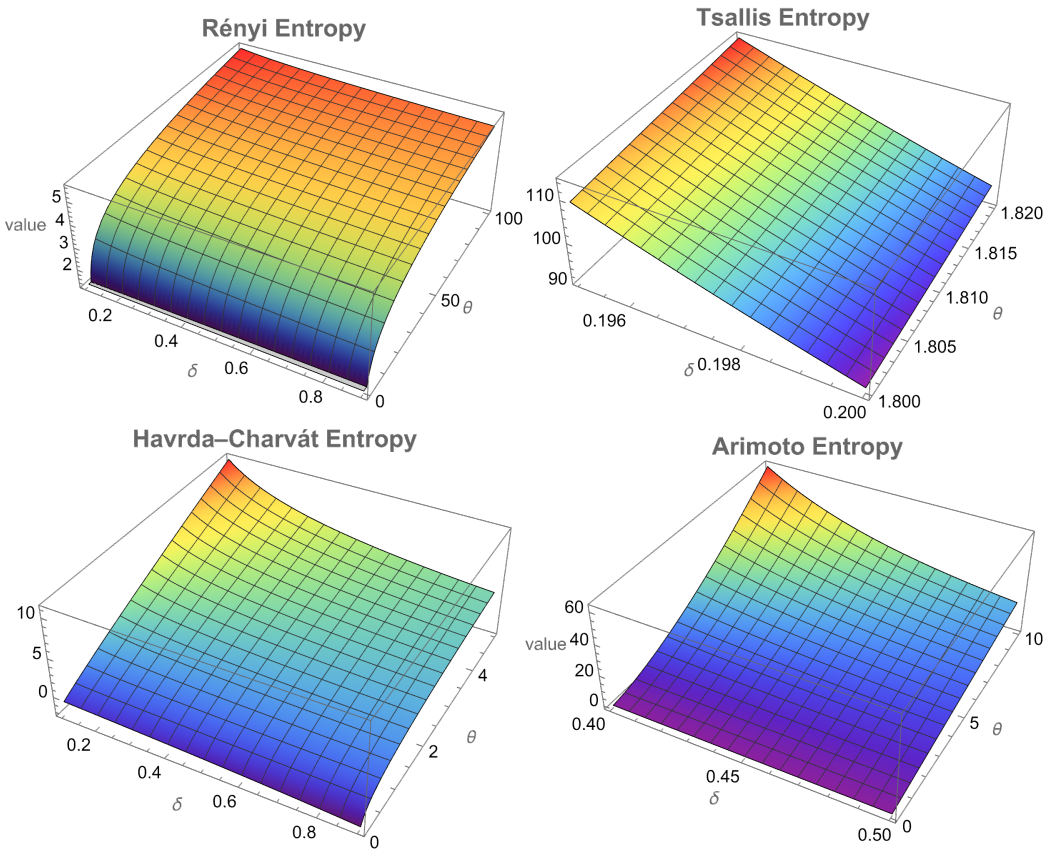

Figure 3. Comparison of different entropy measures for the MMuth distribution.

3. Parameter estimation

Several estimation methods are available for lifetime distributions, each possessing distinct theoretical and practical advantages. In this paper, we focus primarily on estimation procedures that are widely used in reliability and survival analysis and that exhibit strong theoretical properties, such as consistency, efficiency, and robustness to model misspecification. Accordingly, ML and the MPS method are treated as the principal inferential tools.

Additional estimation methods based on goodness-of-fit criteria, including LS, WLS, CvM, and AD estimators, are included for comparative purposes only. These methods are briefly summarized to

assess robustness and sensitivity of the estimates, but they are not intended to replace likelihood-based inference.

3.1. Maximum likelihood estimator

The unknown parameters of the MMuth distribution are estimated using the ML method. Let $x_1, x_2, \ldots, x_n$ be a random sample of n values from the MMuth distribution with parameter θ. The likelihood function is

$$L(\theta) = \prod_{i=1}^{n} f(x_i;\theta) = \left(\frac{1}{2\theta}\right)^n \prod_{i=1}^{n} \left(e^{\frac{x_i}{\theta}} - 1\right)^2 \exp\left(\frac{1}{\theta}\sum_{i=1}^{n} x_i - \sum_{i=1}^{n}\left(e^{\frac{x_i}{\theta}} - 1\right)\right). \tag{3.1}$$

The log-likelihood function for θ can be expressed as

$$\ell(\theta) = -n\log(2\theta) + 2\sum_{i=1}^{n}\log[e^{\frac{x_i}{\theta}} - 1] + \frac{1}{\theta}\sum_{i=1}^{n} x_i - \sum_{i=1}^{n}(e^{\frac{x_i}{\theta}} - 1).$$

The derivative with respect to the unknown parameter θ is given as:

$$\frac{\partial \ell(\theta)}{\partial \theta} = -\frac{n}{\hat{\theta}} - \frac{1}{\hat{\theta}^2}\sum_{i=1}^{n} x_i + \frac{1}{\hat{\theta}^2}\sum_{i=1}^{n} x_i e^{\frac{x_i}{\hat{\theta}}} - \frac{2}{\hat{\theta}^2}\sum_{i=1}^{n}\frac{x_i e^{\frac{x_i}{\hat{\theta}}}}{e^{\frac{x_i}{\hat{\theta}}} - 1} = 0.$$

Substituting $\hat{\theta}_{ML}$, the ML estimator of θ, in (1.5) and (1.6) with general scale parameter $\theta > 0$, we obtain the ML estimator of the SRF and HRF as

$$\hat{S}_{ML}(x) = \frac{1 + \exp[\frac{2x}{\hat{\theta}}]}{2}\exp[-(e^{\frac{x}{\hat{\theta}}} - 1)]$$

and

$$\hat{H}_{ML}(x) = \frac{1}{\hat{\theta}}\frac{(e^{\frac{x}{\hat{\theta}}} - 1)^2 \exp[\frac{x}{\hat{\theta}}]}{1 + \exp[\frac{2x}{\hat{\theta}}]}.$$

3.1.1. Asymptotic interval estimation

The asymptotic CIs for the unknown parameter θ depend on the asymptotic properties of the ML estimators, see [21]. The FI is crucial in asymptotic interval estimation. The FI is defined as $I(\theta) = -\mathbb{E}\left[\frac{\partial^2 \ell(\theta)}{\partial \theta^2}\right]$, and the observed FI is

$$I(\hat{\theta}) = -\frac{\partial^2 \ell(\theta)}{\partial \theta^2}\bigg|_{\theta=\hat{\theta}_{ML}} \quad \text{and} \quad \widehat{\text{Var}}(\hat{\theta}_{ML}) = I^{-1}(\hat{\theta}),$$

where

$$\frac{\partial^2 \ell(\theta)}{\partial \theta^2} = \frac{n}{\theta^2} + \frac{1}{\theta^3}\left(2\sum_{i=1}^{n} x_i - 2\sum_{i=1}^{n} x_i e^{x_i/\theta} + 4\sum_{i=1}^{n}\frac{x_i e^{x_i/\theta}}{e^{x_i/\theta} - 1}\right) - \frac{1}{\theta^4}\left(\sum_{i=1}^{n} x_i^2 e^{x_i/\theta} + 2\sum_{i=1}^{n}\frac{x_i^2 e^{x_i/\theta}}{(e^{x_i/\theta} - 1)^2}\right).$$

Evaluating the observed information at the ML estimator and using the score equation $\partial\ell(\theta)/\partial\theta|_{\theta=\hat{\theta}_{\mathrm{ML}}} = 0$, the second derivative simplifies considerably. In particular, the middle term reduces to $2n/\hat{\theta}^2_{\mathrm{ML}}$, and the observed FI can be written as

$$I(\hat{\theta}_{\mathrm{ML}}) = -\left.\frac{\partial^2\ell(\theta)}{\partial\theta^2}\right|_{\theta=\hat{\theta}_{\mathrm{ML}}} = \frac{2n}{\hat{\theta}^2_{\mathrm{ML}}} - \frac{1}{\hat{\theta}^4_{\mathrm{ML}}}\left(\sum_{i=1}^{n} x_i^2 e^{x_i/\hat{\theta}_{\mathrm{ML}}} + 2\sum_{i=1}^{n}\frac{x_i^2 e^{x_i/\hat{\theta}_{\mathrm{ML}}}}{(e^{x_i/\hat{\theta}_{\mathrm{ML}}}-1)^2}\right).$$

Under standard regularity conditions, the ML estimator is asymptotically normal:

$$\sqrt{n}\,(\hat{\theta}_{ML} - \theta) \xrightarrow{d} N(0,\, I(\theta)^{-1}),$$

where $I(\theta)$ is the FI, $N(0,\, I(\theta)^{-1})$ denotes a normal distribution with mean 0 and variance $I(\theta)^{-1}$, and $\xrightarrow{d}$ denotes the convergence in distribution, as $n \to \infty$.

For the MMuth distribution, the standard regularity conditions for ML estimation are satisfied. The parameter space $\Theta = (0, \infty)$ is open, the PDF is strictly positive and twice continuously differentiable with respect to θ for all $x > 0$, and differentiation under the integral sign is justified by dominated convergence. Moreover, the log-likelihood function is concave in a neighborhood of the true parameter value, ensuring the existence of a unique interior maximizer with probability tending to one as $n \to \infty$. Consequently, the ML estimator is consistent and asymptotically normal, with asymptotic variance given by the inverse FI.

For any $\delta \in (0, 1)$, the $100(1-\delta)\%$ CIs for θ are given as

$$CI_\theta = \left[\hat{\theta} - Z_{\delta/2}\sqrt{\widehat{\mathrm{Var}}(\hat{\theta})},\quad \hat{\theta} + Z_{\delta/2}\sqrt{\widehat{\mathrm{Var}}(\hat{\theta})}\right],$$

where $Z_{\delta/2}$ is the upper $\delta/2$ percentile of a standard normal distribution. To construct CIs for $S(x;\theta)$ and $H(x;\theta)$, we employ the delta method as described in [22, 23]. Let $A_1 = \left[\frac{\partial S(x;\theta)}{\partial\theta}\right]_{\theta=\hat{\theta}_{ML}}$ and $A_2 = \left[\frac{\partial H(x;\theta)}{\partial\theta}\right]_{\theta=\hat{\theta}_{ML}}$ denote the partial derivatives of the SRF and HRF evaluated at the ML estimator. The first derivatives of $S(x;\theta)$ and $H(x;\theta)$ with respect to θ are given by

$$\frac{\partial S(x;\theta)}{\partial\theta} = \frac{x}{2\theta^2}(e^{\frac{x}{\theta}}-1)^2\exp[\frac{x}{\theta} - (e^{\frac{x}{\theta}}-1)]$$

and

$$\frac{\partial H(x;\theta)}{\partial\theta} = -\frac{1}{\theta}\left[\frac{1}{\theta}\frac{\left(e^{\frac{x}{\theta}}-1\right)^2\exp\left(\frac{x}{\theta}\right)}{1+\exp\left(\frac{2x}{\theta}\right)}\right] - \frac{x\exp\left(\frac{x}{\theta}\right)}{\theta^3}\left[\frac{\exp\left(\frac{4x}{\theta}\right)+2\exp\left(\frac{2x}{\theta}\right)-4\exp\left(\frac{x}{\theta}\right)+1}{\left(\exp\left(\frac{2x}{\theta}\right)+1\right)^2}\right].$$

Let $\widehat{\mathrm{Var}}(\hat{\theta}) = I^{-1}(\hat{\theta})$ denote the estimated variance of the ML estimator of θ. Then, by the delta method, the approximate asymptotic variances of $\hat{S}_{ML}(x)$ and $\hat{H}_{ML}(x)$ are given by

$$\widehat{\mathrm{Var}}(\hat{S}_{ML}(x)) = A_1^2\widehat{\mathrm{Var}}(\hat{\theta}) \qquad \text{and} \qquad \widehat{\mathrm{Var}}(\hat{H}_{ML}(x)) = A_2^2\widehat{\mathrm{Var}}(\hat{\theta}).$$

These findings yield the approximate CIs for $S(x;\theta)$ and $H(x;\theta)$ as follows:

$$\left[\hat{S}_{ML}(x) - Z_{\delta/2}\sqrt{\widehat{\mathrm{Var}}(\hat{S}_{ML}(x))},\quad \hat{S}_{ML}(x) + Z_{\delta/2}\sqrt{\widehat{\mathrm{Var}}(\hat{S}_{ML}(x))}\right]$$

and

$$\left[\hat{H}_{ML}(x) - Z_{\delta/2}\sqrt{\widehat{\mathrm{Var}}(\hat{H}_{ML}(x))},\quad \hat{H}_{ML}(x) + Z_{\delta/2}\sqrt{\widehat{\mathrm{Var}}(\hat{H}_{ML}(x))}\right].$$

Unimodality of the log-likelihood. For the one-parameter MMuth distribution, the log-likelihood function $\ell(\theta)$ is twice differentiable and the observed FI $I(\hat{\theta})$ is positive for all $\theta > 0$. Numerical inspection of $\partial^2\ell(\theta)/\partial\theta^2$ across a wide range of θ values and simulated datasets suggests that the log-likelihood is concave in practice. Moreover, the profile log-likelihood plots in Figure 8 exhibit a single, well-defined maximum. Therefore, the ML estimator appears to be unique and corresponds to the global maximum of the log-likelihood function.

3.2. Maximum product spacing

The uniform spacings are defined as

$$D_i(\theta) = F(x_{(i)};\theta) - F(x_{(i-1)};\theta), \qquad i = 1, 2, \ldots, n+1,$$

where $x_{(0)} = 0$, and consequently, $F(x_{(0)};\theta) = 0$, and $x_{(n+1)} = \infty$ with $F(x_{(n+1)};\theta) = 1$. By construction, the spacings sum to unity: $\sum_{i=1}^{n+1} D_i(\theta) = 1$.

The MPS estimator of θ is obtained by maximizing the geometric mean of the spacings:

$$S^*(\theta) = \frac{1}{n+1}\sum_{i=1}^{n+1}\log D_i(\theta).$$

Substituting the CDF of the MMuth distribution gives

$$S^*(\theta) = \frac{1}{n+1}\sum_{i=1}^{n+1}\log\left[\frac{1+\exp[2x_{(i-1)}/\theta]}{2}\exp[-(e^{x_{(i-1)}/\theta}-1)]\right.$$
$$\left. - \frac{1+\exp[2x_{(i)}/\theta]}{2}\exp[-(e^{x_{(i)}/\theta}-1)]\right].$$

The estimating equation for the MPS estimator is obtained by differentiating $S^*(\theta)$ with respect to θ and setting the derivative to zero:

$$\frac{\partial S^*(\theta)}{\partial\theta} = \frac{1}{n+1}\sum_{i=1}^{n+1}\frac{h(x_{(i)};\theta) - h(x_{(i-1)};\theta)}{F(x_{(i)};\theta) - F(x_{(i-1)};\theta)} = 0,$$

where $h(x;\theta) = \partial F(x;\theta)/\partial\theta$ is the derivative of the CDF with respect to θ.

The solution of this non-linear equation yields the MPS estimator $\hat{\theta}_{\mathrm{MPS}}$. In practice, the equation is solved numerically, for instance, by using the `optim` package in R.

3.3. Secondary estimation methods based on goodness-of-fit criteria

For completeness and comparative purposes, we briefly consider several alternative estimation methods derived from goodness-of-fit measures. These are the LS, WLS, CvM, and AD estimators. Such methods are commonly used in distributional fitting but generally lack the optimal efficiency properties of likelihood-based estimators.

In the present context, these estimators are employed to examine the robustness of the proposed model and to provide a benchmark comparison with the primary estimation methods. Due to their secondary role, detailed derivations are omitted, and only the defining estimating equations are provided.

Let $x_{(1)}, \ldots, x_{(n)}$ denote the ordered sample and $F(x;\theta)$ be the CDF of the MMuth distribution.

The LS and WLS estimators minimize

$$\sum_{i=1}^{n} w_i \left\{ F(x_{(i)};\theta) - \frac{i}{n+1} \right\}^2,$$

where $w_i = 1$ for LS estimation and $w_i = [i(n-i+1)]^{-1}$ for WLS estimation.

The CvM estimator is obtained by minimizing

$$\frac{1}{12n} + \sum_{i=1}^{n} \left\{ F(x_{(i)};\theta) - \frac{2i-1}{2n} \right\}^2,$$

while the AD estimator minimizes

$$-n - \frac{1}{n} \sum_{i=1}^{n} (2i-1) \left[\log F(x_{(i)};\theta) + \log(1 - F(x_{(n+1-i)};\theta)) \right].$$

Overall, the inclusion of multiple estimation methods serves to assess the stability and robustness of inference for the MMuth distribution. However, likelihood-based procedures remain the primary tool for statistical inference and interpretation throughout this study.

Uniqueness of solutions. For the secondary estimation methods (MPS, LS, WLS, CvM, AD), the objective functions appear either to be strictly convex (LS, WLS) or lead to unique solutions under the regularity conditions of the MMuth distribution. In all of the following simulation studies with $N = 1000$ replications across various sample sizes and θ values, each optimization algorithm converged to a unique solution without encountering multiple local optima. This numerical evidence supports the practical uniqueness of these estimators.

Remark on entropy and estimation. Although the entropy measures associated with the MMuth distribution depend on a single density-dependent functional, this feature does not impact identifiability or estimation. Entropy functionals summarize global uncertainty properties of the distribution, whereas likelihood-based, spacing-based, and minimum-distance methods rely on the full data likelihood or empirical distribution. The MMuth model, as an identifiable one-parameter scale family, exhibits unimodal log-likelihood and unique solutions for all estimation methods in our extensive numerical experiments. Formal theoretical proofs of these properties, while desirable, are beyond the scope of this empirical study and are noted as a direction for future theoretical work.

4. Numerical study

A Monte Carlo simulation study was conducted to examine the finite-sample performance of the proposed estimation procedures for the MMuth distribution.

Note on scale invariance and simulation design: The MMuth distribution belongs to the scale family, meaning that if $Z \sim \text{MMuth}(1)$, then $X = \theta Z \sim \text{MMuth}(\theta)$. Consequently, for scale-equivariant

estimators, certain performance measures exhibit predictable behavior under scaling: the mean relative error (MRE) and coverage probability (CP) are theoretically invariant to θ, while the root mean squared error (RMSE) and average interval length (AL) scale proportionally with θ. These properties hold asymptotically for consistent estimators.

In finite samples, however, deviations from ideal scaling can occur due to numerical optimization challenges, boundary effects, and higher-order approximation errors. To provide a comprehensive assessment of estimator performance across practically relevant scenarios, we examine multiple values of the scale parameter $\theta \in \{0.5, 1, 2\}$, covering both sub-unitary and supra-unitary scaling. The selected sample sizes $n \in \{50, 75, 100, 150, 500, 1000\}$ span small to large samples, with $n = 75$ and 150 included to capture transitional behavior in the moderate sample range. This design allows us to verify the theoretical scaling properties empirically while also evaluating the robustness and stability of each estimator under varying conditions.

For this purpose, $N = 1000$ independent replications were generated for each combination of sample size and θ value, covering a range of small- to large-sample scenarios and different scale levels.

For each simulated sample, point estimation was performed using ML, MPS, LS, WLS, AD, and CvM estimators. Table 1 reports the average estimate (Est.), the RMSE, and the MRE for all estimates.

Table 1. Estimation results for classical methods.

n	θ	ML			MPS			LS			WLS			AD			CvM		
		Est.	RMSE	MRE	Est.	RMSE	MRE	Est.	RMSE	MRE	Est.	RMSE	MRE	Est.	RMSE	MRE	Est.	RMSE	MRE
50	0.5	0.4992	0.0203	0.0322	0.4944	0.021	0.033	0.5007	0.0242	0.0383	0.5006	0.023	0.0362	0.5008	0.0226	0.0357	0.5002	0.0242	0.0381
50	1	0.9994	0.0404	0.0322	0.9897	0.0416	0.033	1.0025	0.0478	0.0377	1.0023	0.0452	0.0356	1.0023	0.0446	0.0351	1.0014	0.0477	0.0375
50	2	1.9975	0.0833	0.0332	1.9784	0.0859	0.0344	2.0061	0.098	0.039	2.0048	0.0933	0.0371	2.0048	0.092	0.0367	2.0038	0.0977	0.0389
75	0.5	0.4991	0.0169	0.0269	0.4955	0.0174	0.0277	0.5004	0.0199	0.031	0.5001	0.0188	0.0293	0.5002	0.0186	0.0291	0.5000	0.0198	0.031
75	1	0.9982	0.033	0.0265	0.9911	0.034	0.0272	1.0005	0.0383	0.0307	1.0002	0.0363	0.0291	1.0004	0.036	0.0289	0.9998	0.0383	0.0307
75	2	1.9981	0.0654	0.0263	1.9835	0.0669	0.027	2.0013	0.0764	0.0306	2.0011	0.0722	0.029	2.0014	0.0714	0.0288	1.9998	0.0763	0.0306
100	0.5	0.4991	0.0146	0.023	0.4962	0.0151	0.0236	0.5002	0.0167	0.0266	0.5001	0.0158	0.025	0.5001	0.0158	0.0249	0.5000	0.0167	0.0265
100	1	0.9954	0.0289	0.023	0.9896	0.0304	0.0242	0.997	0.0339	0.0269	0.9968	0.032	0.0254	0.9969	0.0317	0.0252	0.9965	0.0339	0.0269
100	2	1.9972	0.0561	0.0227	1.9855	0.0582	0.0233	2.0013	0.0666	0.0269	2.0008	0.0627	0.0254	2.0011	0.0623	0.0252	2.0002	0.0665	0.0268
150	0.5	0.4996	0.0118	0.0186	0.4975	0.0121	0.0191	0.5005	0.0139	0.0222	0.5003	0.0132	0.0209	0.5004	0.0131	0.0208	0.5003	0.0139	0.0221
150	1	1.0002	0.0237	0.0189	0.9958	0.0241	0.019	1.0009	0.0279	0.0223	1.0007	0.0264	0.021	1.0009	0.0262	0.0209	1.0005	0.0279	0.0222
150	2	1.9974	0.0465	0.0185	1.9887	0.0478	0.019	2.001	0.0542	0.0213	2.0004	0.0512	0.0202	2.0006	0.0509	0.02	2.0002	0.0542	0.0213
500	0.5	0.4998	0.0064	0.0104	0.4989	0.0065	0.0106	0.5000	0.0076	0.0121	0.4999	0.0071	0.0114	0.5000	0.0071	0.0114	0.4999	0.0076	0.0121
500	1	0.9999	0.0127	0.0102	0.9982	0.0128	0.0103	1.0005	0.0146	0.0118	1.0003	0.0138	0.0111	1.0004	0.0138	0.0111	1.0004	0.0146	0.0118
500	2	1.9998	0.0258	0.0103	1.9964	0.026	0.0103	1.9998	0.0301	0.0121	1.9999	0.0283	0.0113	2.0000	0.0283	0.0113	1.9996	0.0301	0.0121
1000	0.5	0.4999	0.0045	0.0072	0.4994	0.0045	0.0073	0.5000	0.0054	0.0087	0.5000	0.0051	0.0081	0.5000	0.0051	0.0081	0.5000	0.0054	0.0087
1000	1	1.0000	0.0088	0.007	0.9991	0.0088	0.007	1.0000	0.0103	0.0081	1.0000	0.0097	0.0076	1.0000	0.0097	0.0076	1.0000	0.0103	0.0081
1000	2	1.999	0.0187	0.0075	1.9971	0.0189	0.0076	1.9991	0.0219	0.0088	1.999	0.0206	0.0083	1.9991	0.0206	0.0083	1.999	0.0219	0.0088

The performance measures are defined as

$$\text{MRE}(\theta) = \frac{1}{1000}\sum_{k=1}^{1000}\left|\frac{\widehat{\theta}_k - \theta}{\theta}\right| \quad \text{and} \quad \text{RMSE}(\theta) = \sqrt{\frac{1}{1000}\sum_{k=1}^{1000}(\widehat{\theta}_k - \theta)^2},$$

where $\widehat{\theta}_k$ denotes the estimate obtained from the kth replication.

The results indicate that all estimates are approximately unbiased, with average estimates close to the true parameter values. As expected, RMSE and MRE decrease as the sample size increases, in line with consistency. Absolute RMSE values increase with θ, reflecting the scale nature of the model, while relative errors remain small across all scenarios. Likelihood-based estimators (ML and MPS) also perform well and exhibit rapid convergence as the sample size increases. The goodness-of-fit-based estimators (LS, WLS, AD, and CvM) show comparable performance for moderate to large samples but are slightly less efficient for small sample sizes.

Interval estimation performance is summarized in Table 2, which displays 95% interval estimation based on the ML. For interval assessment, the CP and AL are defined as

$$\text{CP}(\theta) = \frac{1}{1000}\sum_{k=1}^{1000}\mathbb{I}(\theta \in [L_k, U_k]) \quad \text{and} \quad \text{AL}(\theta) = \frac{1}{1000}\sum_{k=1}^{1000}(U_k - L_k),$$

where $[L_k, U_k]$ denotes the interval obtained from the kth replication.

Table 2. CI performance.

n	θ	ML CI		n	θ	ML CI	
		CP	AL			CP	AL
50	0.5	0.938	0.0796	150	0.5	0.944	0.046
50	1	0.946	0.1593	150	1	0.952	0.092
50	2	0.945	0.3185	150	2	0.95	0.1838
75	0.5	0.946	0.065	500	0.5	0.957	0.0252
75	1	0.949	0.1299	500	1	0.954	0.0504
75	2	0.952	0.2601	500	2	0.951	0.1008
100	0.5	0.947	0.0563	1000	0.5	0.949	0.0178
100	1	0.943	0.1122	1000	1	0.95	0.0356
100	2	0.962	0.2251	1000	2	0.945	0.0712

The simulation results show that the ML-based intervals attain near-nominal coverage for moderate to large samples, but they tend to be less accurate in small samples. The simulation results attest to the consistency and improved accuracy of the likelihood-based estimators as the sample size increases.

Figures 4 and 5 show the MRE and RMSE analyses. The visualizations clearly indicate that MRE decreases as sample size increases, which shows better estimator efficiency. Similarly, RMSE

decreases with larger samples, showing improved precision. All analyses were done using the R statistical software.

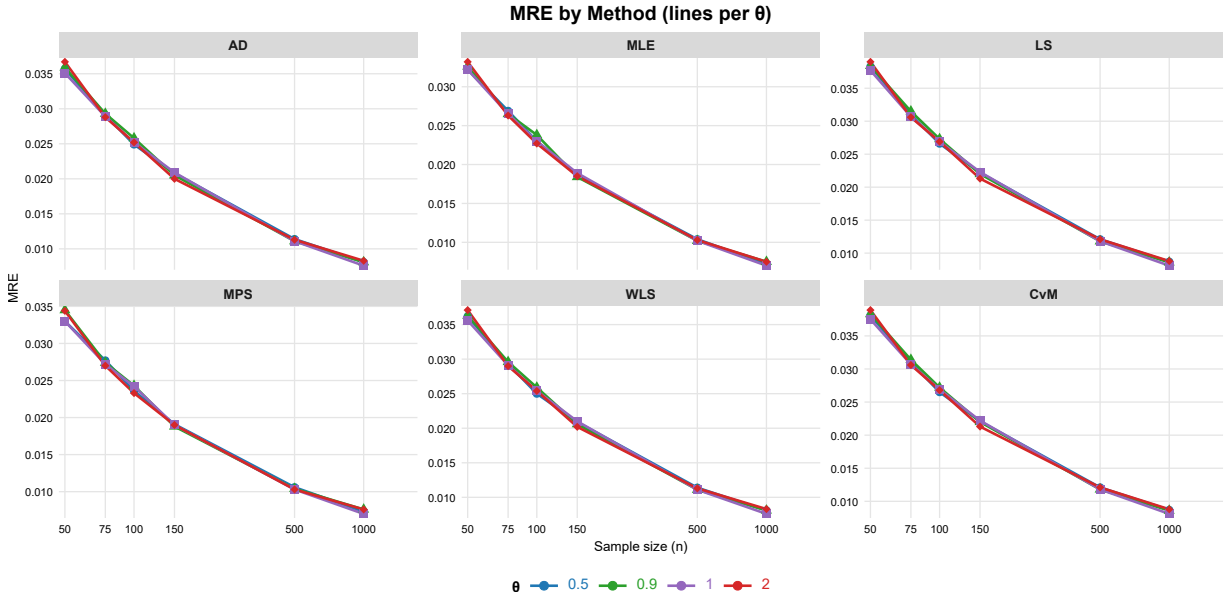

Figure 4. Monte Carlo comparison of the MRE of the proposed estimators for the MMuth distribution under different sample sizes.

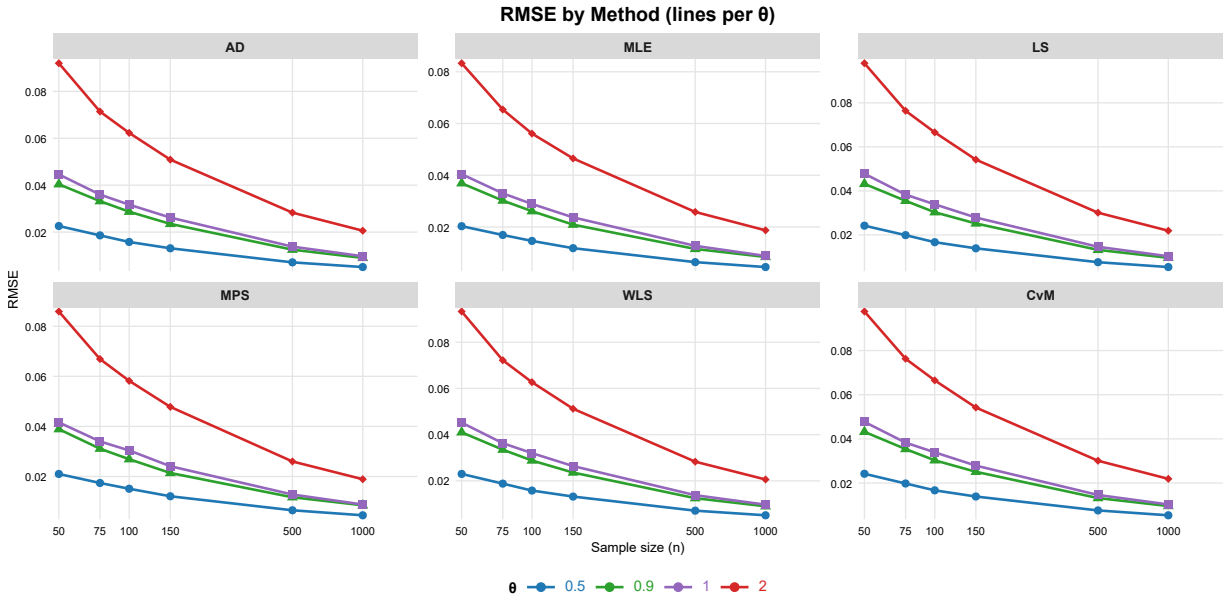

Figure 5. Monte Carlo comparison of the RMSE of the proposed estimators for the MMuth distribution under different sample sizes.

5. Application to a real-world dataset

In this section, the MMuth distribution is evaluated against standard lifetime models using a real-world dataset. Parameters were estimated via ML, and models were compared using goodness-of-fit measures, including the Akaike information criterion (AIC), Bayesian information criterion (BIC), and statistics based on empirical CDFs.

The performance of the MMuth distribution is assessed by applying it to a real-world dataset. The performance of the MMuth model is compared against a range of existing parametric models, with the analysis demonstrating its superior fit in many cases. The following competing models are considered:

- Generalized exponential (GExp) distribution [24],
- Scaled Muth (SMuth) distribution [25],
- Weibull (Wbl) distribution,
- Truncated Muth-Weibull (TMutW) distribution [26],
- Power Lomax (PLom) distribution [27],
- Muth distribution [28],
- Singh-Maddala (SinMad) distribution [29],
- Dagum distribution [30],
- Kies distribution [31],
- Exponentiated Weibull (ExpW) distribution [32],
- Nakagami (Nagam) distribution [33],
- Exponentiated Rayleigh (ExpRay) distribution [34],
- Maxwell (Max) distribution [35].
- Gamma (Gam) distribution.

5.1. The real-world dataset (glass-fiber strengths)

The dataset, sourced from [36], comprises 69 strength measurements (in GPa) for single carbon fibers and impregnated 1000-carbon fiber tows. Table 3 shows that the dataset is slightly leptokurtic and negatively skewed (*mean* < *median*).

Table 3. Descriptive statistics for the dataset.

n	Mean	Median	SD	Min	Max	Skewness	Kurtosis
69	1.4469739	1.4780000	0.5059552	0.0312000	2.5850000	-0.1603059	3.2356301

We estimate the unknown model parameters by the ML method for the dataset. Using those estimates, we obtain the values of the AIC, corrected Akaike information criterion (AICC), BIC, consistent Akaike information criterion (CAIC), and Hannan-Quinn information criterion (HQIC). Moreover, we get the AD statistic (AD-stat) with its corresponding P-value (AD-PV), CvM statistic (CvM-stat) with its corresponding P-value (CvM-PV), and K-S statistic with its corresponding P-value (P-V). According to the goodness-of-fit results in Table 4, with the exception of the classical Muth distribution, most models provided an acceptable fit to the data (i.e., their

P-values are greater than 0.05 for the majority of the goodness-of-fit tests). Among these, the MMuth model is distinguished by having the smallest AIC, AICC, BIC, HQIC, CAIC, and K-S values, as well as the largest p-value. Based on these comprehensive criteria, the MMuth model is recommended as the best model for this dataset. Figures 6–8 show graphical diagnostics for the dataset. The QQ-plot demonstrates that the MMuth distribution closely matches the empirical distribution, with points that are close to the reference line. On the other hand, some competing models exhibit clear differences, especially in the tails. The fitted PDF and CDF of the MMuth distribution in Figure 7 match well with the histogram. Figure 8 also illustrates the stability of the ML estimator, as the profile log-likelihood function behaves well and is unimodal, with a clear peak at the estimated parameter value. These plots confirm the goodness-of-fit statistics, indicating that the MMuth model provides a fit comparable to the competing models.

These results establish the MMuth distribution as a viable alternative, especially for data requiring flexible hazard shapes or nuanced tail behavior.

Table 4. The goodness-of-fit statistics for the dataset.

Dist.	AIC	AICC	BIC	HQIC	CAIC	AD-stat	AD-PV	CvM-stat	CvM-PV	K-S	P-V
MMuth	109.8565	109.9162	112.0906	110.7428	113.0906	0.3168	0.9247	0.0197	0.9974	0.0464	0.9984
TMutW	111.1981	111.5673	117.9004	113.8571	120.9004	0.2976	0.9397	0.0315	0.9717	0.0498	0.9955
PLom	113.9497	114.3190	120.6521	116.6088	123.6521	0.3878	0.8603	0.0419	0.9246	0.0586	0.9719
Wbl	111.9152	112.0971	116.3834	113.6879	118.3834	0.4523	0.7952	0.0567	0.8361	0.0661	0.9239
SinMad	113.9215	114.2908	120.6239	116.5806	123.6239	0.4559	0.7915	0.0575	0.8316	0.0664	0.9213
Dagum	110.6162	110.9854	117.3185	113.2752	120.3185	0.3484	0.8975	0.0404	0.9325	0.0728	0.8576
Kies	110.5439	110.9132	117.2463	113.2030	120.2463	0.4627	0.7844	0.0579	0.8291	0.0738	0.8466
ExpW	111.3913	111.7606	118.0936	114.0504	121.0936	0.4936	0.7527	0.0634	0.7944	0.0787	0.7867
Nagam	117.2998	117.4816	121.7680	119.0725	123.7680	1.0432	0.3351	0.1665	0.3435	0.1004	0.4905
ExpRay	118.5487	118.7306	123.0170	120.3214	125.0170	1.2528	0.2482	0.2047	0.2589	0.1084	0.3918
Max	194.9233	194.9830	197.1574	195.8097	198.1574	1.5516	0.1647	0.2682	0.1666	0.1201	0.2727
Gam	130.3517	130.5335	134.8199	132.1244	136.8199	1.9352	0.0999	0.3090	0.1274	0.1265	0.2193
SMuth	114.2767	114.4585	118.7449	116.0494	120.7449	2.2027	0.0714	0.4154	0.0655	0.1517	0.0836
GExp	139.0738	139.2556	143.5420	140.8464	145.5420	3.0047	0.0274	0.4875	0.0425	0.1443	0.1130
Muth	147.3256	147.3853	149.5597	148.2120	150.5597	21.4697	<0.001	4.3766	<0.001	0.3781	<0.001

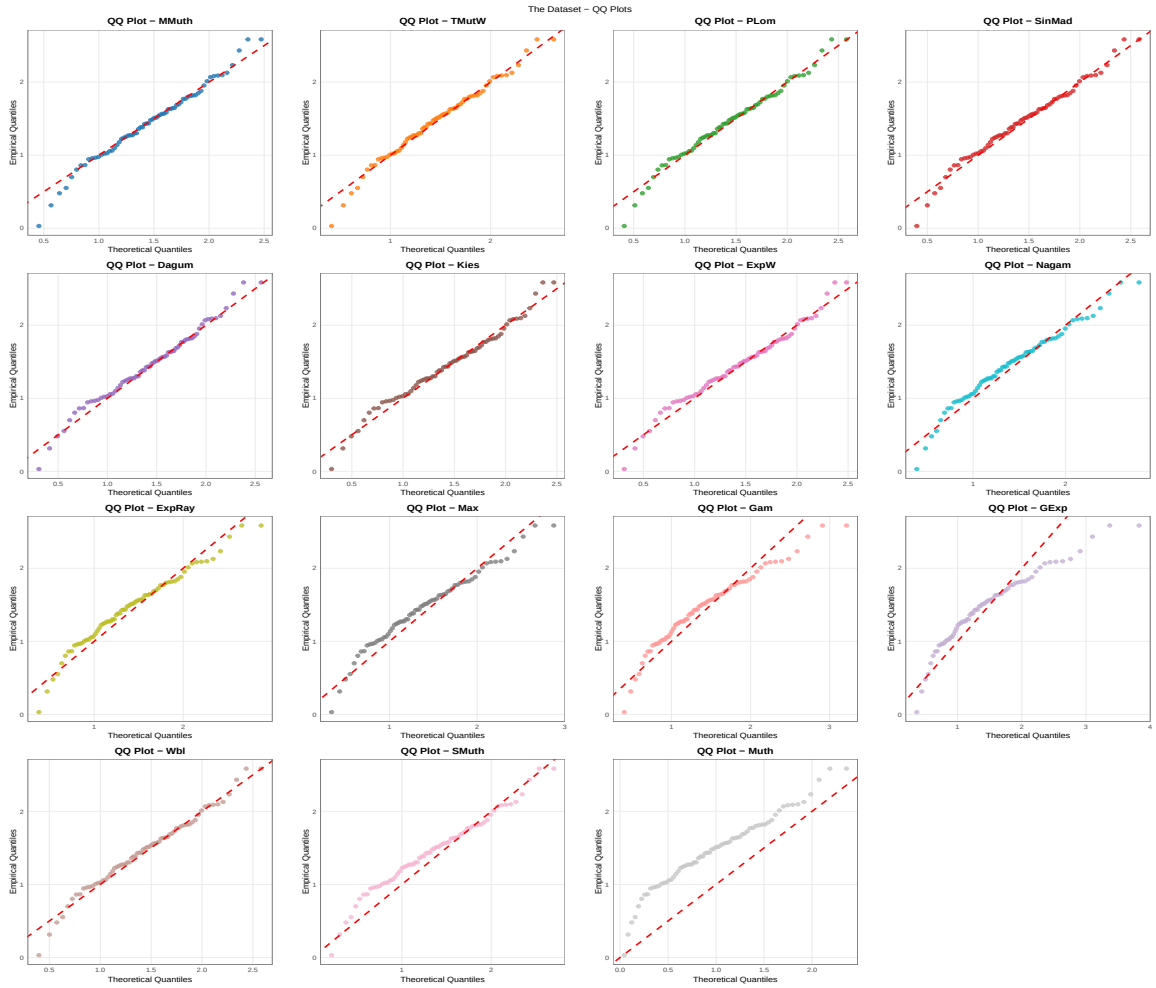

Figure 6. QQ-plots for all competitor models for the dataset.

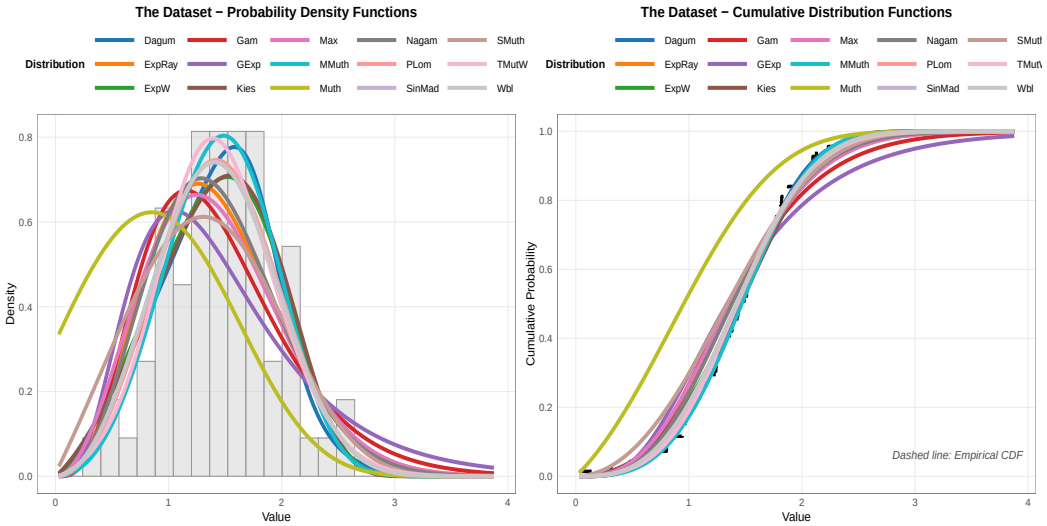

Figure 7. Plots of PDFs and CDFs for all competitor models for the dataset.

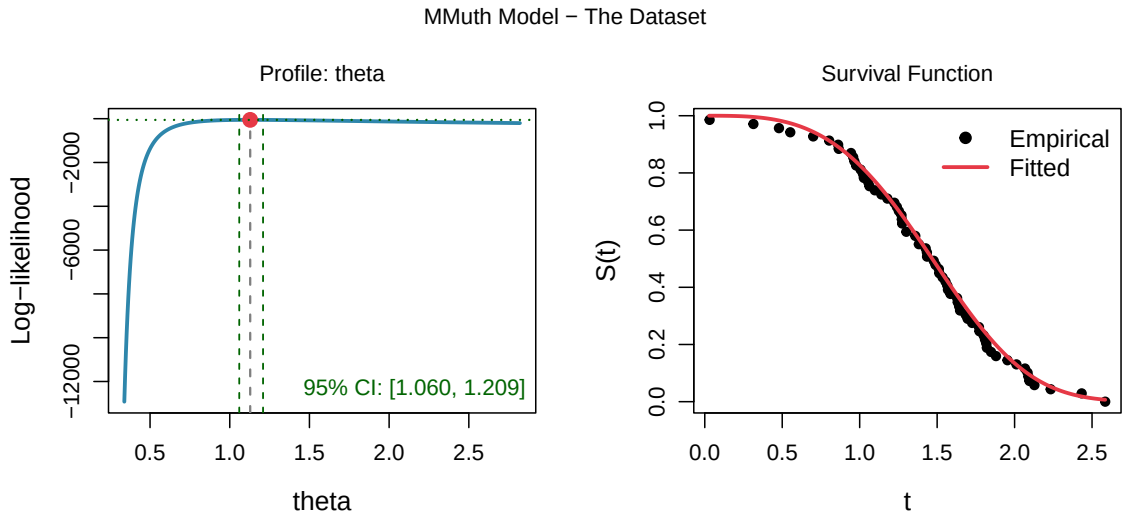

Figure 8. The dataset: profile log-likelihood, its derivative, and SRF under the fitted MMuth distribution.

6. Conclusions and future work

This paper introduced a simple one-parameter modified Muth (MMuth) distribution and outlined its main analytical properties. We looked at several estimation methods and, through extensive simulation studies, showed that the ML estimators give the most accurate point estimates for small samples. Moreover, ML and maximum product of spacings estimators serve as reliable and efficient methods.

When we applied the MMuth distribution to a real-world dataset, it showed a competitive fit compared to many different one-, two-, and three-parameter models. We used AIC, BIC, and standard goodness-of-fit statistics to measure this fit. These results emphasize the benefits of a simpler model when the proposed distribution effectively captures key data features like tail behavior and hazard shape.

The MMuth distribution is subject to certain limitations. As a scale-family distribution with fixed shape properties, it cannot represent complex distribution shapes, especially non-monotonic hazard patterns such as bathtub or unimodal curves, which often appear in reliability settings.

The single-parameter structure, while simple, limits the model's ability to capture both scale and shape changes in complex datasets simultaneously.

Furthermore, this study focused on complete data scenarios. The performance under different censoring methods, which are common in reliability studies, remains an area for future investigation.

Future research should aim to develop bivariate and multivariate extensions of the MMuth distribution. This work could help model joint lifetime data and dependence structures. These extensions might include censoring methods, making them useful in survival and reliability analysis, where incomplete data are often present. Additionally, generalizing the MMuth framework through k-record statistics to derive unit distributions would offer a flexible family for modeling order statistics and record-based stochastic processes. These advancements would expand the use of the MMuth model in various fields, including biomedical research, industrial reliability, and

environmental risk assessment.

Author contributions

H. M. Barakat: Conceptualization and supervision; H. Bakouch: Methodology and formal analysis; M. A. Elgawad: Validation and data curation; H. E. Semary: Visualization; M. A. Alawady: Formal analysis; I. A. Husseiny: Investigation; M. G. Enany: Writing–review & editing; T. S. Taher: Writing–original draft, Formal analysis, and Software.

Use of AI tools declaration

The authors declare they have not used Artificial Intelligence (AI) tools in the creation of this article.

Acknowledgments

The authors are grateful to the editor and anonymous referees for their insightful comments and suggestions, which helped to improve the paper's presentation.

Conflict of interest

The authors declare no conflict of interest.

References

1. K. P. Burnham, D. R. Anderson, *Model selection and multimodel inference: A practical information-theoretic approach*, New York: Springer, 2002. https://doi.org/10.1007/b97636
2. E. J. Muth, Reliability models with positive memory derived from the mean residual life function, *Theor. Appl. Reliab.*, **2** (1977), 401–435.
3. P. Jodrá, M. D. Jiménez-Gamero, M. V. Alba-Fernández, On the Muth distribution, *Math. Model. Anal.*, **20** (2015), 291–310. https://doi.org/10.3846/13926292.2015.1048540
4. L. M. Leemis, J. T. McQueston, Univariate distribution relationships, *Am. Stat.*, **62** (2008), 45–53. https://doi.org/10.1198/000313008x270448
5. Z. He, S. Wang, J. Shi, D. Liu, C. Duan, Y. Shang, Physics-informed neural network supported wiener process for degradation modeling and reliability prediction, *Reliab. Eng. Syst. Safe.*, **258** (2025), 110805. https://doi.org/10.1016/j.ress.2025.110906
6. Z. He, S. Wang, D. Liu, A degradation modeling method based on artificial neural network supported Tweedie exponential dispersion process, *Adv. Eng. Inform.*, **65** (2025), 103376. https://doi.org/10.1016/j.aei.2025.103376
7. Z. He, S. P. Wang, D. Liu, A nonparametric degradation modeling method based on generalized stochastic process with B-spline function and Kolmogorov hypothesis test considering distribution uncertainty, *Comput. Ind. Eng.*, **203** (2025), 111036. https://doi.org/10.1016/j.cie.2025.111036

8. J. F. Lawless, *Statistical models and methods for lifetime data*, John Wiley & Sons, 2011. https://doi.org/10.1002/9781118033005
9. G. P. Patil, C. R. Rao, The weighted distributions: A survey of their applications, *Appl. Stat.*, 1977, 383–405.
10. G. P. Patil, C. R. Rao, Weighted distributions and size-biased sampling with applications to wildlife populations and human families, *Biometrics*, **34** (1978), 179–189. https://doi.org/10.2307/2530008
11. M. Alam, H. M. Barakat, H. S. Bakouch, C. Chesneau, Order statistics and record values moments from the Topp-Leone Lomax distribution with applications to entropy, *Wireless Pers. Commun.*, **135** (2024), 2209–2227. https://doi.org/10.1007/s11277-024-11136-w
12. J. M. Amigó, S. G. Balogh, S. Hernández, A brief review of generalized entropies, *Entropy*, **20** (2018), 813. https://doi.org/10.3390/e20110813
13. F. Lad, G. Sanfilippo, G. Agro, Extropy: Complementary dual of entropy, *Statist. Sci.*, **30** (2015), 40–58. https://doi.org/10.1214/14-sts430
14. M. A. Alawady, H. M. Barakat, T. S. Taher, I. A. Husseiny, Measures of extropy for k-record values and their concomitants based on Cambanis family, *J. Stat. Theory Pract.*, **19** (2025), 11. https://doi.org/10.1007/s42519-024-00423-1
15. R. A. Aldallal, H. M. Barakat, M. S. Mohamed, Exploring weighted Tsallis extropy: Insights and applications to human health, *AIMS Math.*, **10** (2025), 2191–2222. https://doi.org/10.3934/math.2025102
16. H. M. Barakat, M. A. Alawady, T. S. Taher, I. A. Husseiny, Second-order concomitants of order statistics from bivariate Cambanis family: Some information measures and estimation, *Commun. Stat. Simul. C.*, **54** (2025), 3195–3221. https://doi.org/10.1080/03610918.2024.2344023
17. M. Nagy, H. M. Barakat, M. A. Alawady, I. A. Husseiny, A. F. Alrasheedi, T. S. Taher, et al., Inference and other aspects for q-Weibull distribution via generalized order statistics with applications to medical datasets, *AIMS Math.*, **9** (2024), 8311–8338. https://doi.org/10.3934/math.2024404
18. C. Tsallis, Possible generalization of Boltzmann-Gibbs statistics, *J. Stat. Phys.*, **52** (1988), 479–487. https://doi.org/10.1007/BF01016429
19. J. Havrda, F. Charvát, Quantification method of classification processes: Concept of structural α-entropy, *Kybernetika*, **3** (1967), 30–35.
20. S. Arimoto, Information measures and capacity of order α for discrete memoryless channels, In: *Topics in Information Theory*, 1977.
21. I. A. Husseiny, H. M. Barakat, T. S. Taher, M. A. Alawady, Fisher information in order statistics and their concomitants for Cambanis bivariate distribution, *Math. Slovaca*, **74** (2024), 501–520. https://doi.org/10.1515/ms-2024-0038
22. W. H. Greene, The econometric approach to efficiency analysis, In: *The Measurement of Productive Efficiency and Productivity Change*, 2008. https://doi.org/10.1093/acprof:oso/9780195183528.003.0002
23. S. G. Nassr, T. S. Taher, T. Alballa, N. M. Elharoun, Reliability analysis of the Lindley distribution via unified hybrid censoring with applications in medical survival and biological lifetime data, *AIMS Math.*, **10** (2025), 14943–14974. https://doi.org/10.3934/math.2025670

24. D. Kundu, R. D. Gupta, Generalized exponential distribution: Bayesian estimations, *Comput. Stat. Data Anal.*, **52** (2008), 1873–1883. https://doi.org/10.1016/j.csda.2007.06.004

25. A. Saroj, P. K. Sonker, S. Kumari, R. Ranjan, M. Kumar, Parameter estimation of scale Muth distribution (SMD) under type-I censoring using classical and Bayesian approaches, *Reliab. Theor. Appl.*, **18** (2023), 429–445.

26. A. M. Almarashi, F. Jamal, C. Chesneau, M. Elgarhy, A new truncated Muth generated family of distributions with applications, *Complexity*, **2021** (2021), 1211526. https://doi.org/10.1155/2021/1211526

27. A. S. Hassan, M. Abd-Allah, On the inverse power Lomax distribution, *Ann. Data Sci.*, **6** (2019), 259–278. https://doi.org/10.1007/s40745-018-0183-y

28. P. Jodrá, H. W. Gomez, M. D. Jimenez-Gamero, M. V. Alba-Fernandez, The power Muth distribution, *Math Model. Anal.*, **22** (2017), 186–201. https://doi.org/10.3846/13926292.2017.1289481

29. K. Kakamu, Simulation studies comparing dagumand Singh-Maddala income distribution, *Comput. Econ*, **48** (2016), 593–605. https://doi.org/10.1007/s10614-015-9538-z

30. H. S. Mohammed, M. Nassar, R. Alotaibi, A. Elshahhat, Analysis of adaptive progressive type-II hybrid censored dagum data with applications, *Symmetry*, **14** (2022), 2146. https://doi.org/10.3390/sym14102146

31. P. Chandra, Y. M. Tripathi, L. Wang, C. Lodhi, Estimation for Kies distribution with generalized progressive hybrid censoring under partially observed competing risks model, *P. I. Mech. Eng. O J. Ris.*, **237** (2023), 1048–1072. https://doi.org/10.1177/1748006x221122570

32. G. S. Mudholkar, D. K. Srivastava, Exponentiated Weibull family for analyzing bathtub failure-rate data, *IEEE T. Reliab.*, **42** (1993), 299–302. https://doi.org/10.1109/24.229504

33. K. Kumar, R. Garg, H. Krishna, Nakagami distribution as a reliability model under progressive censoring, *Int. J. Syst. Assur. Eng. Manag.*, **8** (2017), 109–122. https://doi.org/10.1007/s13198-016-0494-3

34. Q. Gong, R. Chen, H. Ren, F. Zhang, Estimation of the reliability function of the generalized Rayleigh distribution under progressive first-failure censoring model, *Axioms*, **13** (2024), 580. https://doi.org/10.3390/axioms13090580

35. R. Goel, M. M. Abdelwahab, M. M. Hasaballah, Bayesian analysis of the Maxwell distribution under progressively type-II random censoring, *Axioms*, **14** (2025), 573. https://doi.org/10.3390/axioms14080573

36. M. G. Bader, A. M. Priest, Statistical aspects of fibre and bundle strength in hybrid composites, In: *Progress in science and engineering of composites*, 1982, 1129–1136.